Gallium Nitride Photocathode Development for Imaging Detectors

Oswald H.W. Siegmund[a], Anton S. Tremsin[a], John V. Vallerga[a], Jason B. McPhate[a], Jeffrey S. Hull[a], James Malloy[a] and Amir M. Dabiran[b]

[a] Univ. of California, Berkeley, Space Sciences Laboratory, Berkeley, CA, USA 94720-7450;
[b] SVT Associates Inc, 7620 Executive Drive, Eden Prairie, MN 55344

ABSTRACT

Recent progress in Gallium Nitride (GaN, AlGaN, InGaN) photocathodes show great promise for future detector applications in Astrophysical instruments. Efforts with opaque GaN photocathodes have yielded quantum efficiencies up to 70% at 120 nm and cutoffs at ~380 nm, with low out of band response, and high stability. Previous work with semitransparent GaN photocathodes produced relatively low quantum efficiencies in transmission mode (4%). We now have preliminary data showing that quantum efficiency improvements of a factor of 5 can be achieved. We have also performed two dimensional photon counting imaging with 25mm diameter semitransparent GaN photocathodes in close proximity to a microchannel plate stack and a cross delay line readout. The imaging performance achieves spatial resolution of ~50μm with low intrinsic background (below 1 event sec^{-1} cm^{-2}) and reasonable image uniformity. GaN photocathodes with significant quantum efficiency have been fabricated on ceramic MCP substrates. In addition GaN has been deposited at low temperature onto quartz substrates, also achieving substantial quantum efficiency.

Keywords: Gallium nitride, Photon counting, microchannel plate, detector, photocathode.

1. INTRODUCTION

Many future and potential NASA missions in astrophysics, solar physics, planetary physics, Earth observation, and a number of other disciplines utilize the performance of photon counting sensor systems. One of the key enabling technologies of these sensor systems is their detection efficiency, which depends on the performance of the photocathodes used to convert the incoming radiation into photoelectrons. The window and substrate for the photocathode material, and the detection scheme for the emitted photoelectrons are also key parameters.

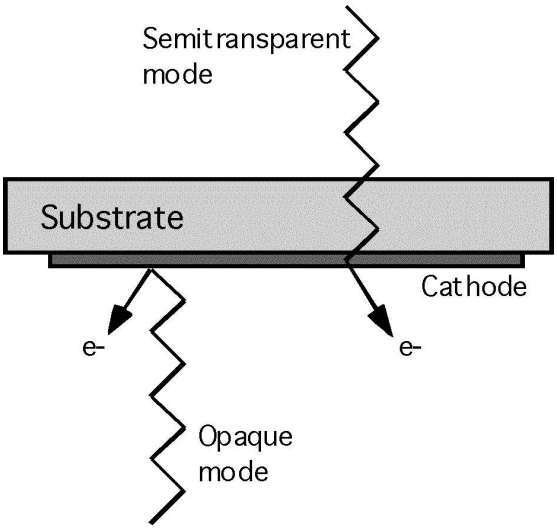

Figure 1. Schematic of semitransparent and opaque photocathode operation for a cathode coated substrate.

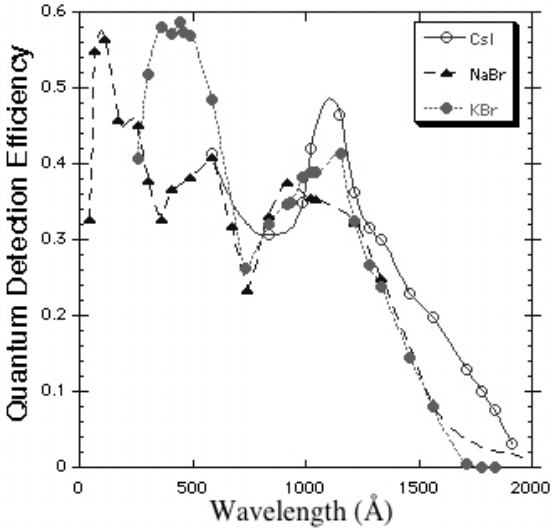

Figure 2. QDE vs. wavelength for CsI, NaBr and KBr opaque cathodes coated on MCPs [1,2].

Not only is the efficiency important for the future instruments, but the photocathode stability, radiation hardness, life-time, background rate, and out of bandpass rejection are also crucial for the success of future missions. Semitransparent (photoemission from the surface opposite the illumination surface) and opaque (photoemission from the same side as the illumination) photocathodes are both of interest (Fig. 1). CsI (Fig. 2) is a frequently used UV photocathode, as are a number of other alkali halide materials. Semitransparent CsTe and opaque diamond have also been used (Fig. 3), but none of these match the efficiency and bandwidth of GaN.

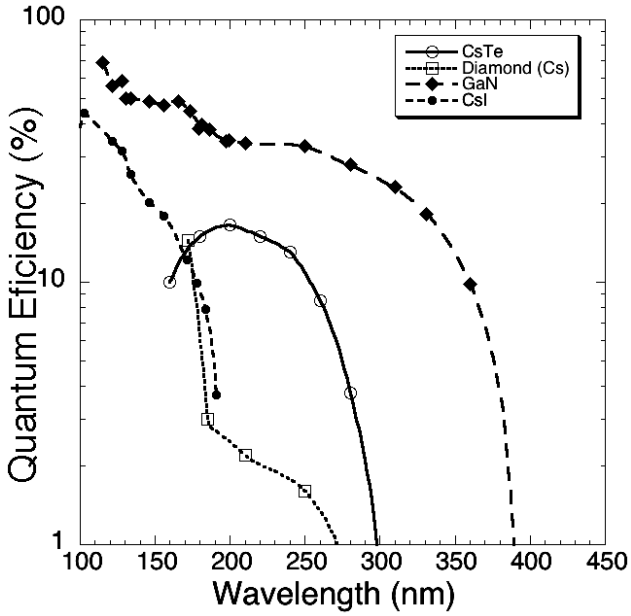

Figure 3. Comparison of different ultraviolet cathodes CsI on MCPs, opaque GaN and diamond[3], and CsTe.

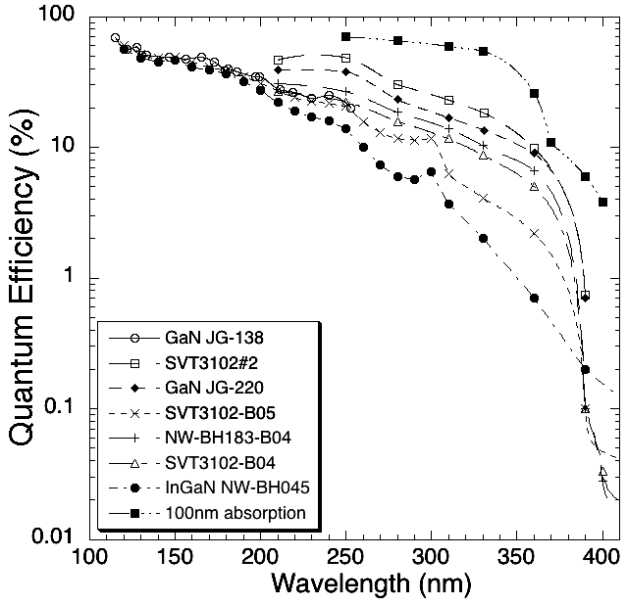

Figure 4. Summary of our previous[4,5,6,7,8] GaN/InGaN QE measurements for various samples & processes.

The nitride-III semiconductors, and specifically GaN (band gap energy 3.5 eV), AlN (band gap 6.2 eV) and their alloys $Al_xGa_{1-x}N$, are potentially attractive as UV photocathodes for position sensitive detector systems. These can provide a broad coverage in the 150-400 nm wavelength regime between alkali halide photocathodes (<200 nm), and the various optical photocathodes (>400 nm, multi-alkali and GaAs). CsTe is often used as a far ultraviolet semitransparent cathode, but has a fairly low efficiency (<20%), and cuts off at <300 nm. CsTe is also highly sensitive to, and irreversibly damaged by, gas exposure. Recent studies performed by our group [4,5,6,7,8] as well as other reports [9 -17] indicate that Cs activated GaN cathodes can be more robust and may possibly achieve >50% QDE from the MgF_2 window cutoff to ~350 nm. An attractive feature of GaN photocathodes is their ability to be tuned with respect to the long wavelength cutoff. Variation of the AlN and GaN ratio can be used in order to fine tune the sensitivity cutoff, and in the same fashion this can be accomplished with InGaN (Fig. 4). Benjamin et al[9] have also reported negative electron affinity for $Al_xGa_{1-x}N$, with x ~0.7-0.75. Meanwhile, Machuca et al[10] have reported high GaN QEs (25% at 256 nm) using Cs:O activation, and show evidence that activated GaN should be much more robust than GaAs as a stable photoemitter. Tereshchenko et al [14] reported 25% efficiency of Cs:O activated GaN photocathodes at 250 nm. Most recently Mizuno et al [18] have reported 25% efficiency at 240 nm for semitransparent GaN working in a MCP sealed tube with a phosphor readout. Our previous [6] investigations of opaque mode GaN cathodes (Fig. 4) have shown high QE at wavelengths below ~240nm. The QE at longer wavelengths is highly dependent on the surface preparation and activation conditions to produce negative electron affinity (Fig. 4). The long wavelength limit for GaN cathodes is found to be at ~380nm – 390nm, where the QE drops off rapidly by several orders of magnitude. For InGaN the QE dropoff is much slower and extends to longer wavelengths without a steep dropoff in QE (Fig. 4). Our current efforts are focused on implementing GaN photocathodes for use in photon counting imaging detectors as well as continuing to optimize and enhance the GaN QE.

2. UV PHOTOCATHODES

2.1 GaN photoemission and stability

The attenuation characteristics of crystalline GaN material allow the layer thickness required to efficiently absorb UV (100 nm-400 nm) photons to be calculated. Optical constant data [11,12] indicates that the optimal thickness of the film should be between 100 and 200 nm. Ideally, all photons would interact in the GaN layer as close to the emission surface as possible. Thus the electrons created would all be close to the exit surface and be efficiently emitted from the surface when activated to achieve negative electron affinity. In practice the attenuation length[12] of photons in GaN increases with increasing wavelength and increases sharply at the band edge where GaN becomes transparent. These data also indicate reflectivity of ~20% relatively independent of wavelength and incident angle. Nemanich et al.[19] concluded that the minority carrier diffusion length in this material is ~200nm, sufficient to transport most of the photoelectrons through thinner cathodes. To further increase the probability of electrons reaching the emitting surface a thin (10nm - 30nm) barrier layer of AlN is deposited directly on the substrate to create a potential barrier at the GaN/substrate boundary. The general optimization strategy for sample materials combines factors of substrate matching, dopant concentration, barrier layers and thickness. The relative merits of using opaque (front surface illumination and emission) and semitransparent (substrate side illumination and GaN front surface emission) depend largely on the achievable QE and the logical constraints of the device geometry. Both scenarios were evaluated in our investigation since they each have specific applications, and the combined data give useful diagnostics of the cathodes.

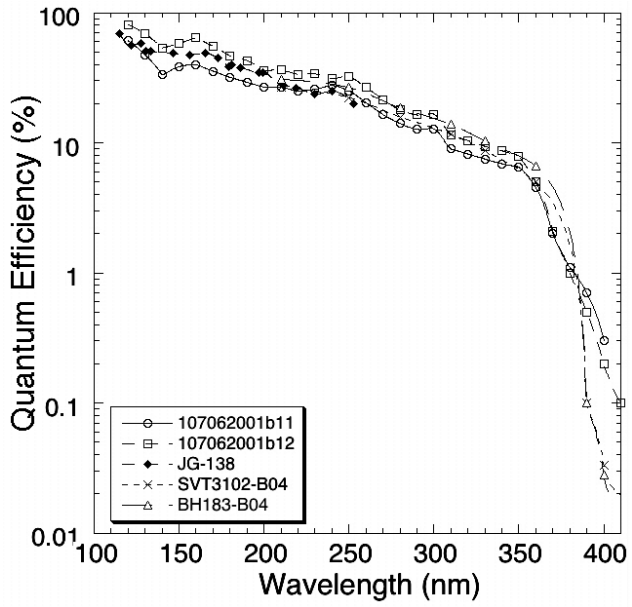

Figure 5. QDE vs. wavelength for opaque GaN cathodes. Recent data for 150nm opaque GaN on sapphire (107062001). Graded P doping with $>10^{19}$ cm^{-3} near substrate, ~30nm AlN base layer, (b11, b12 two different bakeout processes).

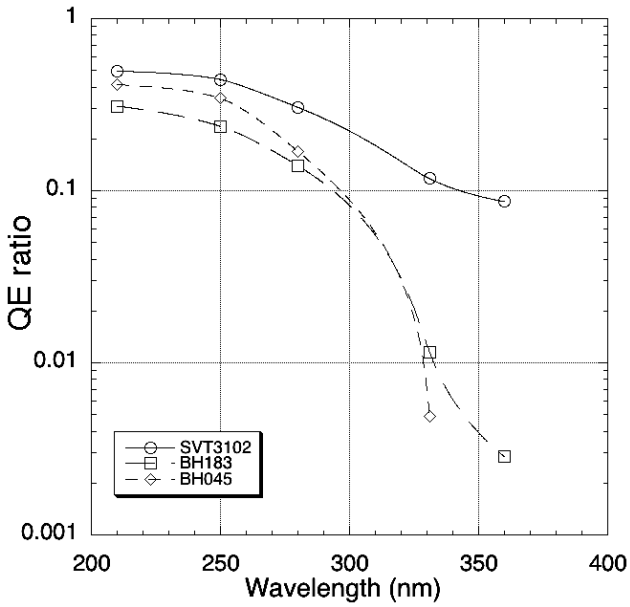

Figure 6. Ratio of GaN QE. (After exposure to 760 Torr N_2 and a 250°C vacuum bake / the initial QE). SVT3102 MBE 120nm GaN (P doped 10^{17} cm^{-3}), BH183 CVD 660nm GaN, BH045 CVD 500nm InGaN.

Assessment of GaN photocathode materials has been done using 2" sapphire wafers with GaN deposited by molecular beam epitaxy (MBE) at SVT associates. The cathode samples are typically diced into 1cm squares for processing and measurement. Our test chamber allows measurements to the MgF_2 cutoff and also the angular dependence, opaque and semitransparent QE all in the same environment. Based on the crystalline structure of GaN, we have normally used C-plane sapphire for the substrate material as it is a good match for CVD or MBE deposition of GaN films. The SVT samples have a thin "reflective" layer of AlN (~10 - 30nm nm) and a 100 nm to 250 nm GaN top layer Mg (p) doped. The latest samples evaluated all include higher (10^{19} /cm^3) P dopant (Mg) concentrations than those we have tried before, as well as depth graded doping profile. The latter samples ware designed to have the extraction electric field by the engineered band bending mechanism suggested and experimentally tested by Yang et al.[20] for GaAs photocathodes. In their

measurements the quantum efficiency of depth graded GaAs photocathode was superior to all previous results due to the enhanced escape probability of the photoelectron from the photocathode surface into vacuum. We have also made substantial progress in the consistency of our cleaning and surface activation techniques, resulting in good repeatability of the achievable photocathode performance. Key factors in cathode activation include cleaning techniques, degassing, vacuum baking/cleaning and surface activation with alkali metal (Cs, Cs:O). Many of these issues have been investigated[4,5,6,7], resulting in a basic process that has repeatedly achieved good photocathode performance in our ultrahigh vacuum chamber sample test facility. Recent results (Fig. 5) show consistent QE for opaque cathode operation. Many samples have also been completely re-processed several times, with slightly better results for second pass cesiation. The higher P (Mg) doped depth graded samples (with $>10^{19}$ cm^{-3}) seem to have slightly better efficiency than earlier samples with lower dopant concentrations ($<10^{18}$ cm^{-3}). Our measurements also indicate that the thinner samples (100nm to150nm GaN) with high P dopant (with $>10^{19}$ cm^{-3}) give the best results, but that the cleaning and processing conditions are more critical for the achievement of high QEs.

Stability and robustness of the GaN cathodes is important to their application in detectors. We have been able to clean, reprocess and activate samples numerous times and achieve the same QE results. Other measurements (Fig. 6) of GaN show that after air or nitrogen exposure, we can recover most of the GaN QE by a simple vacuum bakeout (250° C), and fully re-establish QEs by further cesiation of the cathode. A cathode sample in a sealed tube[6] made in collaboration with ITT and Northwestern University has also enabled us to measure long term stability of GaN photocathodes. This sample was monitored over >4 years, and shows no measurable QE degradation, thus encouraging our expectations of the robustness of GaN. The long wavelength response of GaN cathodes has also been measured (Fig. 7) and shows an initial steep drop at ~380nm followed by a less rapid decrease above 400nm. InGaN shows only a gradual decrease.

2.2 GaN cathode substrates and deposition techniques

GaN photocathodes are typically grown on a matching crystal lattice sapphire or silicon carbide substrate with C-plane at the surface. It was assumed that the quality of films would be substantially degraded if they were not grown on a planar surface of a matching crystalline lattice, and if the substrate temperature was not maintained at the high temperatures needed (~700°C). SVT have made trial depositions of polycrystalline GaN films onto fused silica substrates at temperatures below 350°C which we have subsequently cleaned, processed and activated.

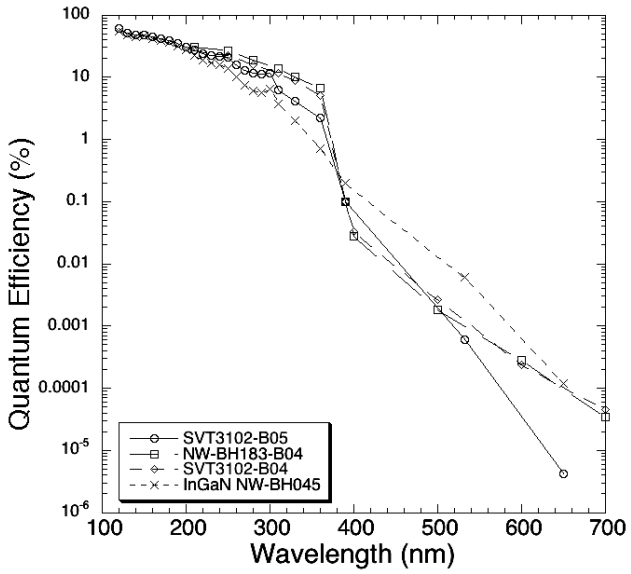

Figure 7. QDE vs. wavelength for opaque GaN/InGaN. BH183 CVD 660nm GaN, BH045 CVD 500nm InGaN. SVT3102 MBE 120nm GaN (P doped 10^{17} cm^{-3}).

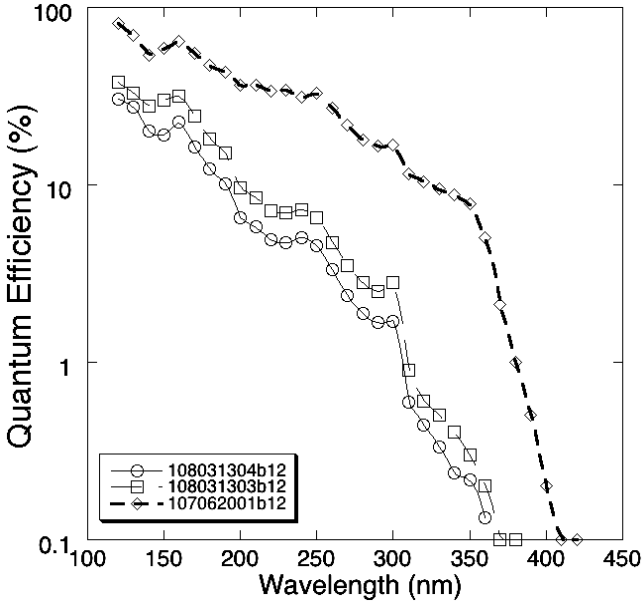

Figure 8. QE vs. wavelength for GaN deposited on fused silica (108031303/4) at low temperature (<350°C). compared with 150nm GaN on sapphire (107062001).

The QE results for these GaN cathodes (Fig. 8) is substantially below our typical results for GaN on sapphire. However the QE is still significant, and greater than CsI above wavelengths of 150nm. There are a number of possible reasons why the QE is degraded. Optimization of the deposition process at low temperature to establish the best GaN layer structure, and the dopant concentration, will have to be studied. In addition we performed a very mild cleaning process to the samples in our first processes. Since cleaning plays a large part in the QE performance we expect that the QE will improve with more aggressive cleaning procedures. The initial result is thus encouraging, both in that the GaN can be deposited onto poorly matched substrates, and that the deposition temperature can be reduced allowing a wider range of potential substrates.

In collaboration with Synkera Technologies Inc. we have been examining structured ceramic substrates and their potential application as MCPs. Several of these alumina MCP substrates have also been deposited with thick (0.5µm) polycrystalline GaN. These have either, no holes, or 25µm holes on 50µm centers (25% open area). These samples were processed and cesiated in exactly the same way as the sapphire-GaN substrates, then measurements of the QE were made. Sample results are included in Fig. 9, and show that a solid substrate (without holes) has poor opaque QE and a short cutoff wavelength. However the sample with holes is substantially better, with >20% QE at 120nm. From angular variation measurements we believe the improved QE is attributable to the hole/cathode combination. The photoelectron escape probability is higher for opaque cathodes at grazing angles and thus the QE is higher, as we normally find for MCPs with alkali halide opaque cathodes. Given the poor substrate open area ratio (25% OAR), we are achieving substantial QE from an unoptimized substrate/GaN layer. The implication is that a QE curve for opaque GaN on a larger (>60%) open area ratio Al_2O_3 substrate would be proportionally better. Again further work is in progress to optimize this possibility and investigate the relevant fabrication and processing techniques.

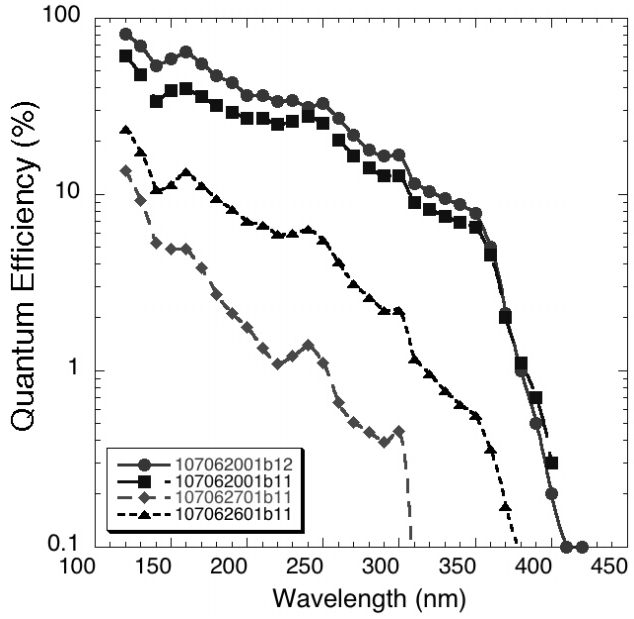

Figure 9. Opaque QE vs. wavelength for 500nm GaN on Alumina substrates (107062701 solid alumina substrate, 107062601 – substrate with 25µm holes) compared with 150nm GaN (107062001 [two thermal procedures]).

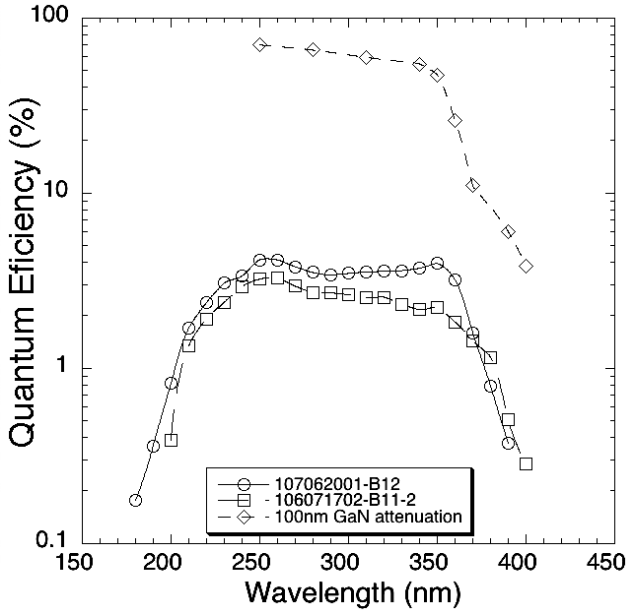

Figure 10. QDE vs. wavelength for semitransparent GaN. 150nm GaN (107062001), 100nm GaN (106071702), both on sapphire, 30nm AlGaN, P doped up to 2 x 10^{19} cm^{-3}.

2.3 GaN semitransparent cathodes

In addition to our studies of opaque GaN QE we have also measured most samples in semitransparent mode. The flat top QE response (Fig. 10) from 200nm to 400nm is expected (short end cutoff due to sapphire and AlN absorption of UV), but the QE is consistently only 3 to 4% QE, compared with the >60% photon absorption in the GaN layer (Fig. 10). However, Fuke et al.[17] report that QE as high as 25% can be achieved. Our samples with depth graded P dopant with high P doping near the substrate are slightly better than the high surface graded P doped samples. Functionally, short wavelengths (that produce higher photoelectron energies) are absorbed closer to the incident (substrate) surface of

the GaN requiring the electrons produced to travel further in the GaN before escaping. They are thus attenuated and have less energy when they reach the GaN surface. Longer wavelengths penetrate further and produce electrons closer to the GaN emitting surface. With the existing data it is difficult to separate the effects of poor surface escape probability from poor electron transport. However, we have since found that much more efficient semitransparent cathodes may be achieved with thinner layers (see **3.** below), and additional information suggests that field enhancement of GaN can produce significant electron transport improvements[21].

3. GAN PHOTOCATHODE MCP IMAGING DETECTORS

To assess the imaging qualities of GaN photocathodes, and the practicality of constructing photon counting imaging detectors with GaN photocathodes, we have constructed a test detector (Fig. 11). The detector uses 25mm diameter semitransparent GaN photocathodes on sapphire substrates in close proximity (0.5mm) to a microchannel plate stack and a cross delay line readout. This detector is almost identical to devices we have used for a number of other applications[22]. The design uses a Sapphire/GaN semitransparent cathode in a holder (Fig. 12). Due to the three clip wires used to hold down the substrate in the GaN deposition process, three "shadows" can be seen on the otherwise uniformly colored GaN coating (Fig. 12) (purple for 100nm GaN and green for 150nm GaN). All samples have P doping with about 10^{19} cm^{-3} and an AlN 30nm layer on the substrate. Fig. 11 shows the MgF_2 entrance window with the GaN sample in its holder placing the GaN close (<0.5mm) to a MCP stack that is read out with a cross delay line anode. The objectives of this effort were demonstration of the GaN cathode efficiency and spatial uniformity of response, verification of the low background for GaN cathodes, and demonstration of 2D imaging properties. Fig. 13 shows one sample installed into the detector, and Fig. 14 shows a close up of the 150nm GaN sample in its holder.

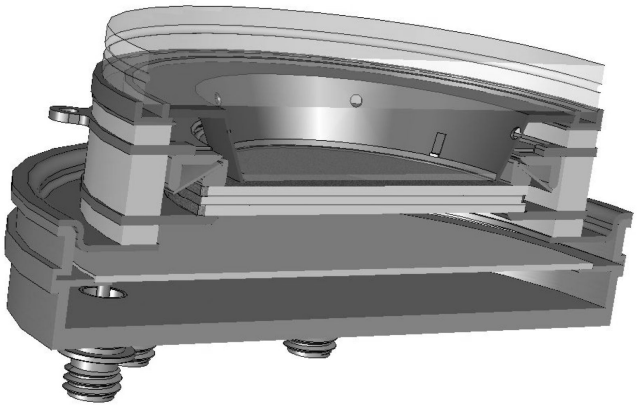

Figure 11. Cutaway schematic of a photon counting imaging detector with MgF_2 input window, GaN on sapphire in proximity with a "Z" stack of microchannel plates (MCPs) and a cross delay line readout.

Figure 12. 25mm GaN coated sapphire window mounted in a holder that puts the GaN close (0.5mm) to the MCP surface. Notice the three shadows where wire clips were used to hold the substrate when the GaN was deposited.

The gain and pulse height for single photon detection was very good (6 x 10^6 gain, 50% FWHM). Fully illuminated images (Fig. 15) of the 100nm GaN sample show the shadow of a tool wire (upper left), and the three GaN fabrication wire shadows. The general uniformity of the response is reasonable (Fig. 17), but there are defects which can be seen. These are directly related to damage in the cathode layer which can be seen under careful microscope examination. The image for the 150nm GaN sample is shown in Fig. 16. It too shows defects in the GaN layer but is generally more uniform. Quite small defects are visible given the spatial resolution of ~50µm which is achieved using ~120v cathode to MCP bias. Note the defect in the lower right in Fig.14 is seen in the image at the bottom of Fig. 16. So clearly more work on optimizing layer damage is needed. What is also very obvious is the very high response (5x higher than the

general QE) in the thin layers where the mounting wires shadowed the GaN depositions (Fig. 17). This is consistent for all of the samples and indicates that our optimization should be to consider thinner GaN layer. Thus, we trade off the attenuation of light in the GaN, but allow higher escape probability for photoelectrons. The indications are that the

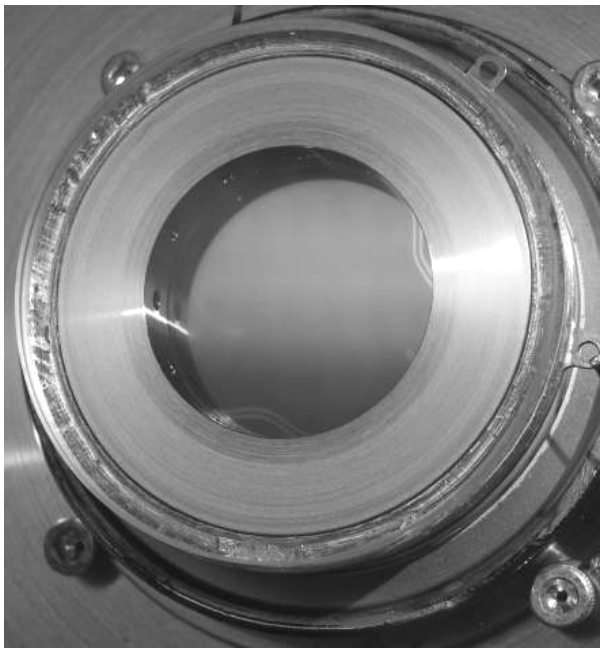

Figure 13. GaN sample mounted in holder installed into imaging detector just inside Indium seal for MgF_2 window.

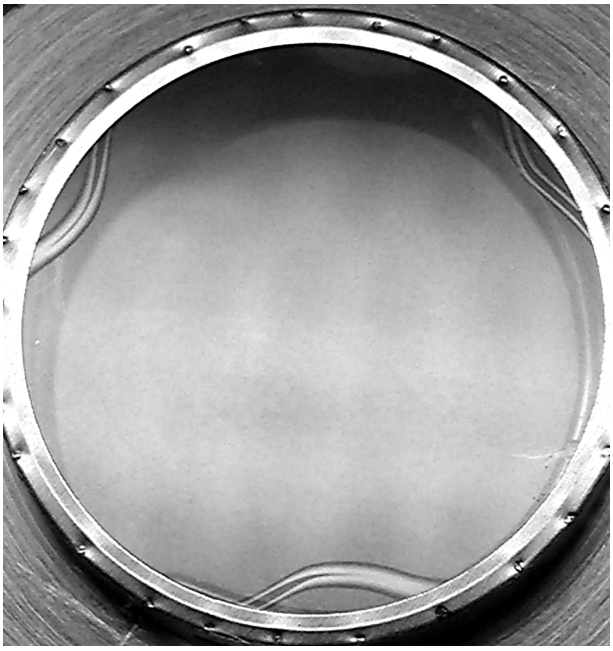

Figure 14. 150nm GaN layer 25mm sample in holder. Note wire clip shadows and defect mark on lower right.

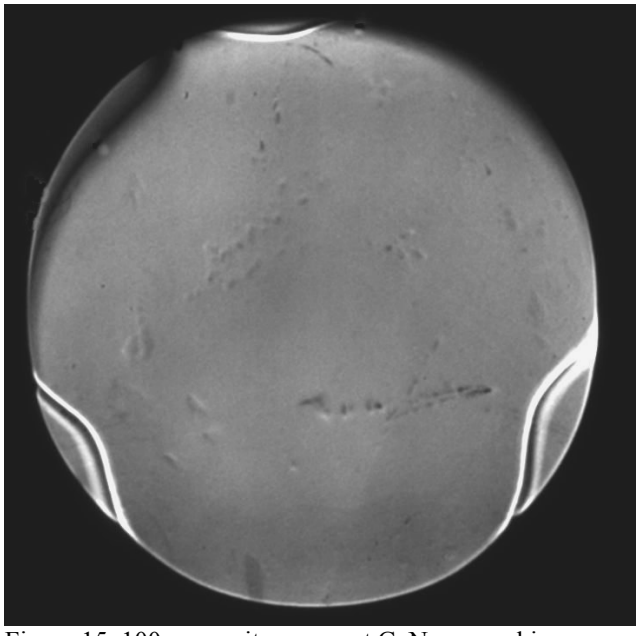

Figure 15. 100nm semitransparent GaN on sapphire. Image with 10^8 events. 254nm UV illumination, 60V bias. Note dark shadow of mounting hardware – upper left, also high clip wire shadow response, and image defects.

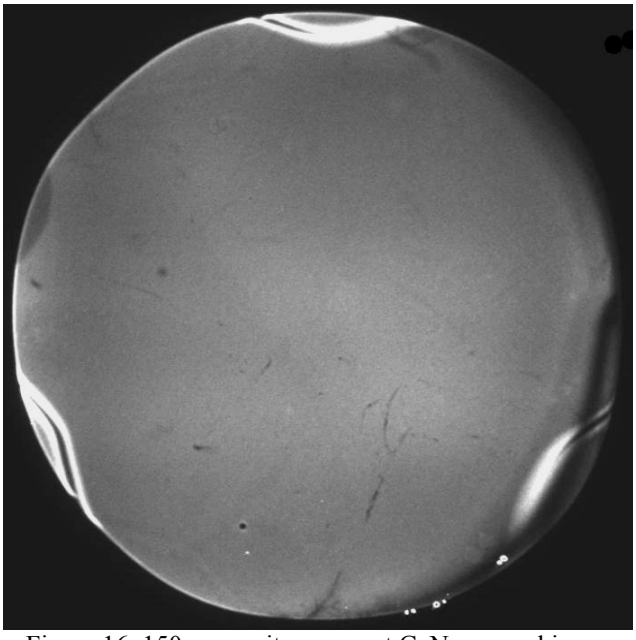

Figure 16. 150nm semitransparent GaN on sapphire, image with 10^8 events. 254nm UV light, 120V bias. Note dark shadow of mounting hardware – lower right, also high clip wire shadow response, and image defects.

higher QE areas are achieving closer to 20% QE as compared with our typical results of 3% to 4% with these GaN layers. This seems to be similar to the data recently reported by Mizuno et al [18] of 25% QE at ~240nm wavelength. In ongoing work we are re-optimizing our GaN depositions to provide a uniformly higher QE semitransparent layer. Lastly, we have made measurements of the background event rate in photon counting mode (Fig. 18). The spatial distribution of background events is essentially uniform. The intrinsic background rate for the MCP detector, measured with the GaN cathode biased off was ~0.5 event cm^{-2} sec^{-1} while the background rate for the detector with the GaN cathode biased on (120V) was ~ 1 event cm^{-2} sec^{-1}. Thus the effective GaN background contribution was ~0.5 event cm^{-2} sec^{-1}. This is higher than most UV photocathodes and is likely due to the smaller bandgap of GaN resulting in a low level of thermionic emission. Investigation of cooling the cathode should confirm this, but for most applications this background is sufficiently low to not pose a problem.

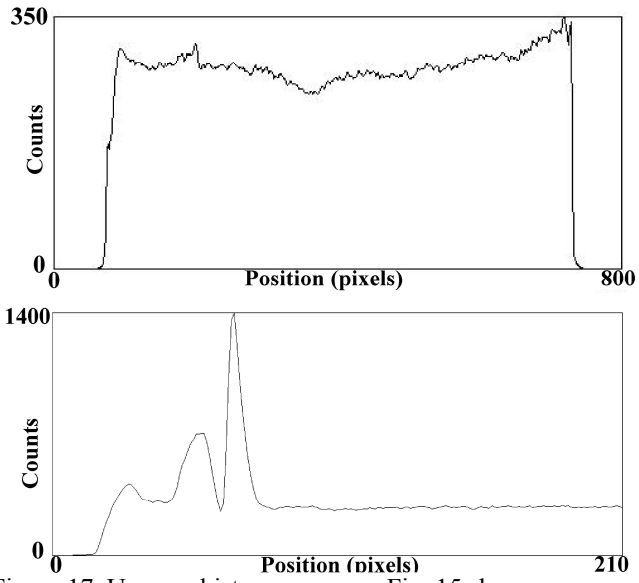

Figure 17. Upper – histogram across Fig. 15 shows response uniformity of 100nm GaN. Lower – histogram through Fig. 15 at wire clip location showing QE enhancement.

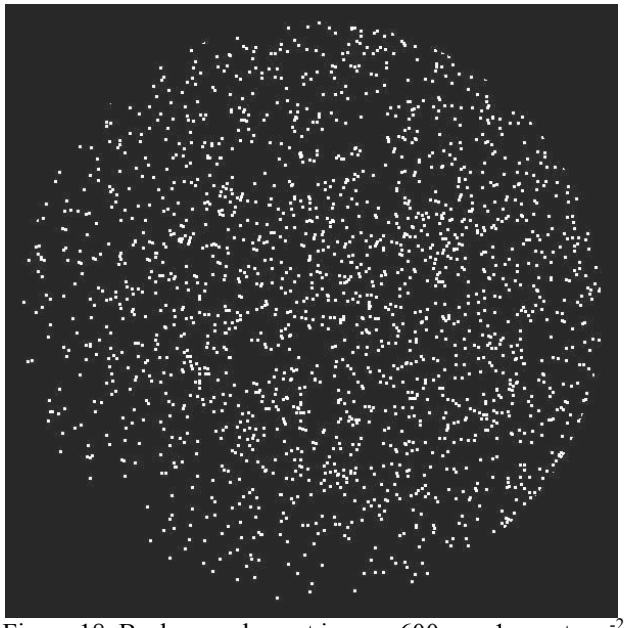

Figure 18. Background event image, 600 sec, 1 event cm^{-2} sec^{-1}. 100nm semitransparent GaN on 25mm sapphire. Same sample as Fig. 15, 120V GaN cathode bias.

ACKNOWLEDGMENTS

The authors wish to thank Dr. D. Routkevitch at Synkera Technologies Inc. for providing alumina MCP substrates. We would also like to thank Prof. M. Ulmer and Prof. B. Wessels at Northwestern University for providing MOVPE GaN materials. The studies presented here were performed through NASA grants NNG06GD46G, NAG5-12710 and NAG511547.

REFERENCES

1. Siegmund, O.H.W. E. Everman, J. Vallerga, J. Sokolowski, and M. Lampton, "Ultraviolet Quantum Detection Efficiency of Potassium Bromide as an Opaque Photocathode Applied to Microchannel Plates", *Applied Optics*, **26(17)**, 3607 - 3614 (1987).
2. Siegmund, O. H. W., Gaines, Geoffrey A., "Photoelectron energy spectra of opaque photocathodes in the extreme and far ultraviolet", SPIE, Vol. A92-20226 06-35. p. 217-227 (1990).
3. Tremsin A.S., Siegmund O.H.W., "UV Photoemission Efficiency of Polycrystalline CVD Diamond Films", Diamond and Related Materials, **14** (N1), 48-53 (2005).
4. Siegmund, O. H.W. Tremsin, A. S.; Martin, A; Malloy, J; Ulmer, M. P.; Wessels, B, GaN photocathodes for UV detection and imaging, SPIE, **5164**, 134-143 (2003).

5. Siegmund, O. H. W.; Vallerga, John V.; McPhate, Jason B.; Tremsin, Anton S. Next generation microchannel plate detector technologies for UV astronomy, SPIE, **5488**, 789-800 (2004).
6. Siegmund O, Vallerga J., McPhate J., Malloy J., Tremsin A., Martin A., Ulmer M., Wessels B., „Development of GaN photocathodes for UV detectors", Nucl. Instr. Meth., A **567**, 110-113 (2006).
7. Siegmund O., Vallerga J., Tremsin A., McPhate J., "Microchannel plates: recent advances in performance", SPIE, **6686**, 66860W (2007).
8. Ulmer M. P., Wessels B. W., Han B., Gregie J., Tremsin A. S. and Siegmund O. H. W., "Advances in Wide-Band-Gap Semiconductor Based Photocathode Devices for Low Light Level Applications", Proc. SPIE, **5164**,144-154 (2003).
9. Benjamin MC, Bremser MD, Weeks TW, et al., "UV photoemission study of heteroepitaxial AlGaN films grown on 6H-SiC", Applied Surface Science, **104**, 455-460 (1996).
10. Machuca F., Liu Z., Sun Y., Pianetta P., Spicer W. E., Pease R. F. W., "Oxygen species in Cs/O activated gallium nitride (GaN) negative electron affinity photocathodes", J. Vac. Sci. Technol., **B 21**(4), 1863-1869 (2003).
11. Munoz M, Huang YS, Pollak FH, Yang H, "Optical constants of cubic GaN/GaAs(001): Experiment and modeling", J. App. Phys., **93**(5), 2549-2553 (2003).
12. Muth J. F., Brown J. Dd., Johnson M. A. L., Zhonghai Yu, Kolbas R. M., Cook J. W., Jr. and Schetzina J. F., "Absorption coefficient and refractive index of GaN, AlN and AlGaN alloys", J. Nitride Semicond. Res., 4S1, G5. (1999).
13. Norton, Timothy J.; Woodgate, Bruce E.; Stock, Joseph; Hilton, George; Ulmer, Melville P.; Aslam, Shahid; Vispute, R. D., "Results from Cs activated GaN photocathode development for MCP detector systems at NASA GSFC", Proc. SPIE, **5164**, 155-164 (2003).
14. Tereshchenko O. E., Shaibler G. E., Yaroshevich A. S., Shevelev S. V., Terekhov A. S., Lundin V. V., Zavarin E. E., and Besyul'kin A. I., "Low-Temperature Method of Cleaning p-GaN(0001) Surfaces for Photoemitters with Effective Negative Electron Affinity", Phys. of the Solid State, **46**(10), 1881-1885 (2004).
15. Stock J; Hilton, G.; Norton, T.; Woodgate, B.; Aslam, S.; Ulmer, M. Progress on development of UV photocathodes for photon-counting applications at NASA GSFC, Proc. SPIE, **5898**, 95-102 (2005)
16. Qiao J., Chang B., Yang Z., Tian S., Gao Y., "Comparative study of GaN and GaAs photocathodes" Proc SPIE, **6621**, 66210K (2008).
17. Fuke S., Sumiya M., Nihashi T., Hagino M., Matsumoto M., Kamo Y., Sato M.,Ohtsuka K., "Development of UV-photocathodes using GaN film on Si substrate", Proc SPIE, **6894**, 68941F (2008).
18. Mizuno, I. T. Nihashi, T. Nagai, M. Niigaki, Y. Shimizu, K. Shimano, K. Kato, T. Ihara, K. Okano, M. Matsumoto, M. Tachino, "Development of UV image intensifier tube with GaN photocathode".Proc. SPIE **6945**-54, (2008).
19. Nemanich RJ, Baumann PK, Benjamin MC, Nam OH, Sowers AT, Ward BL, Ade H, Davis RF, Applied Surface Science, **132**, 694-703 (1998)
20. Yang Z., Chang B., Zou J., Qiao J., Gao P., Zeng Y., and Li H., "Comparison between gradient-doping GaAs photocathode and uniform-doping GaAs photocathode", Appl. Optics, **46,** 7035-39 (2007).
21. Foutz, B.E, L.F. Eastman, U.V. Bhapkar, and M.S. Shur, Applied Physics Lett., **70**, 2849, (1997)
22. Siegmund, O. H. W. "Advances in microchannel plate detectors for UV/visible Astronomy", Proc. SPIE, **4854** (2002).